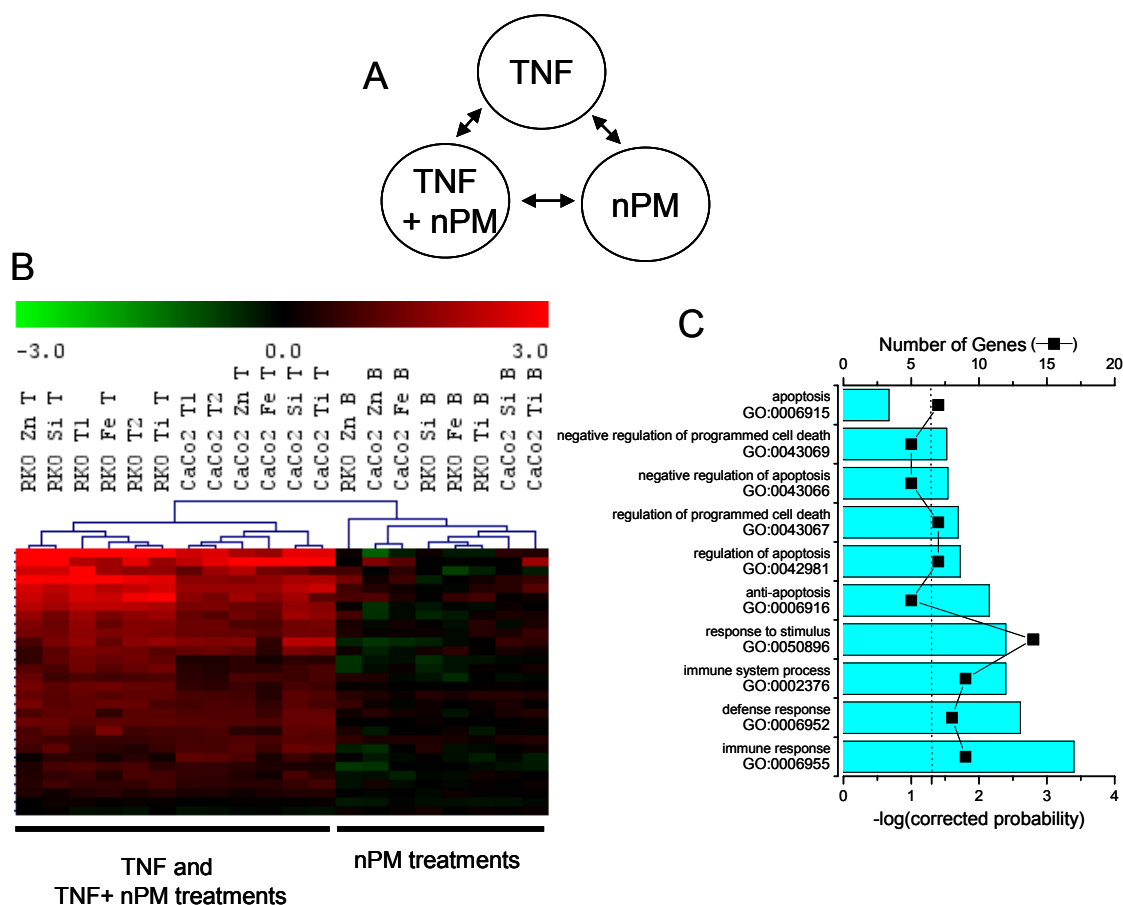


## Supplemental methods and data for “Responses of human cells to ZnO nanoparticles: a gene transcription study.” by Moos et al.

### Microarray results: General nanoparticle transcriptional responses.

To evaluate if there was a non-specific transcriptional effect of the nanoparticles we first compared BSA pretreated RKO or CaCo-2 colon cancer cells to cells treated with TNF- $\alpha$ , nanoparticulate only, or TNF- $\alpha$  plus nanoparticulate by whole genome expression analysis. If TNF- $\alpha$  had an effect on the cellular responsiveness to nanoparticles in these cell lines, we expected to observe potentiation of the metal oxide response.



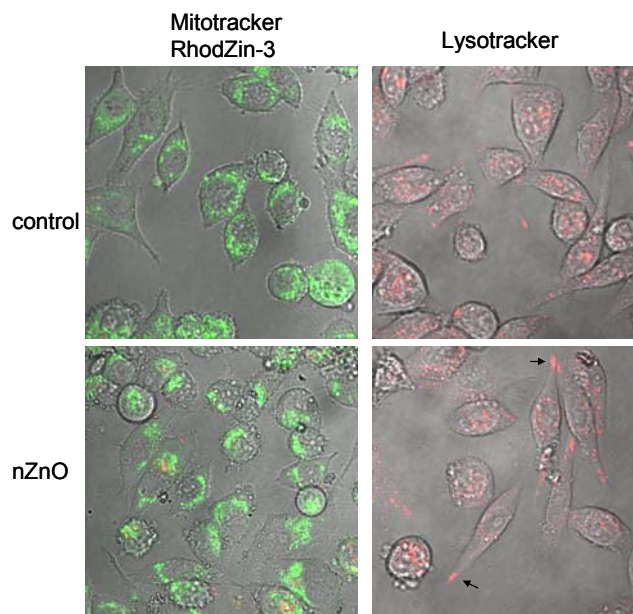
**Figure S1.** Hierarchical cluster visualization of TNF- $\alpha$  dominated transcript profiles when evaluating broad treatment categories. **(A)** Schematic of the multiclass SAM. This analysis evaluated gene expression differences among the following categories: 1) TNF- $\alpha$  pretreatment (denoted with T1 or T2), 2) nanoparticle treatment (denoted Zn for ZnO; Ti for TiO<sub>2</sub>; Fe for Fe<sub>2</sub>O<sub>3</sub>; and Si for SiO<sub>2</sub>), and 3) TNF- $\alpha$  plus nanoparticle treatment. The samples are coded with a B for BSA and a T for the TNF- $\alpha$  co-treatment. **(B)** The complete unique geneset is represented in the heatmap and shows the clustering of samples into TNF- $\alpha$  treatments and non-TNF- $\alpha$  treatments. Using a median false discovery rate of 0%, 54 elements, representing 36 distinct probes, or 30 unique genes were identified. **(C)** The top ten gene ontology (GO) categories (biological processes or molecular functions) as determined by EASE analysis with the Bonforonni corrected

probability (cyan bars) and the number of genes that identified the gene ontology category (■) are displayed. The dashed line represents significance at the  $p=0.05$  level for reference in the corrected probabilities. The majority of the genes identified (a complete list is in the gene expression supplementary tables) are consistent with NF- $\kappa$ B induction.

### Confocal Microscopy and Flow cytometric analysis

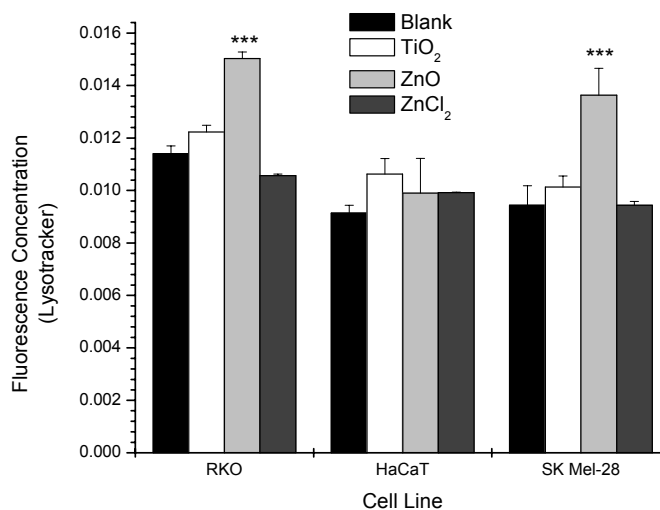
RKO cells were seeded on chamber coverslip slides for confocal microscopy. The cells were treated with  $10 \mu\text{g}/\text{cm}^2$  nanoZnO or nanoTiO<sub>2</sub> for 24 hrs. The cells were incubated with 100 nM Mitotracker Green and 100 nM RhodZin-3 or 100 nM Lysotracker to visualize effects on subcellular compartmentalization using the University of Utah cell imaging core facility.

**Figure S2.** Control (top) and ZnO (bottom) treatments of Mitotracker and RhodZin-3 (left) and Lysotracker (right). Little RhodZin-3 staining is observed to co-localize with the mitochondria (yellow signal represents overlapping signal). ZnO treatment does increase Lysotracker staining in the periphery of the cells (arrows) similar to the observation of membrane whorls and structures in the TEM images (figure 3).



We also used Lysotracker for in a cytometric assay to determine if there was a change in the total amount of lysosomes following ZnO or TiO<sub>2</sub> treatment. Cells were incubated with media, TiO<sub>2</sub>, ZnO (nanomaterial at  $10 \mu\text{g}/\text{cm}^2$ ), or 100  $\mu\text{M}$  ZnCl<sub>2</sub> for 24 hrs and then incubated with 100 nM Lysotracker. Cells were seeded into 6-well plates at a density of  $\sim 2 \times 10^5$  cells/well and allowed to grow overnight. Following treatment, cells were trypsinized, centrifuged at  $250\times g$  for 5 minutes, and resuspended in 1 ml phosphate buffered saline (PBS). Cells were then centrifuged at  $250\times g$  for 5 minutes and resuspended in a fresh 1 ml of  $1\times$  PBS. Lysotracker fluorescence concentration was then determined using a Beckman Cell Lab Quanta SC flow cytometer by dividing the fluorescence for each cell by its measured electronic volume. For each assay, a minimum of 10,000 events per sample were recorded.

**Figure S3.** Quantification of fluorescence concentration of lysotracker in RKO, HaCaT, and SK Mel-28 cells. ZnO treatment in the RKO and SK Mel-28 cells displayed



significant increases in lysosomes/cell (\*\*\*,  $p < 0.001$ ).

While no discrete differences were observed in the mitochondria, these data indicate that ZnO promoted lysosome formation which could be consistent with autophagy.

### Autophagy immunoblot analysis

The best characterized biochemical marker of autophagy is LC3B cleavage. We measured the ZnO-mediated autophagic response using immunoblot analysis of RKO, HaCaT and SK Mel-28 cells. Cells in 6-well plates were placed on ice. Media was aspirated and cells were then washed with 1ml of cold  $1 \times$  PBS, the PBS aspirated, and protein lysates were prepared. Protein concentrations were determined using Bradford reagents. Absorbance at 595 nm was measured using a Perkin-Elmer VictorV3. Proteins were separated by NuPAGE 10% or 4-12% Bis-Tris gels, and transferred to a polyvinyl difluoride membrane.

Membranes were blocked with 5% nonfat dry milk in TBS-T and then probed for LC3B (1:1000) with rabbit polyclonal antibody (Sigma). Peroxidase conjugated secondary antibodies (1:5000) were used in conjunction with chemiluminescence detection to evaluate protein expression. Protein was detected using Western Lightning Western Blot Chemiluminescence reagent, visualized, and quantified using a Kodak Image Station 440.

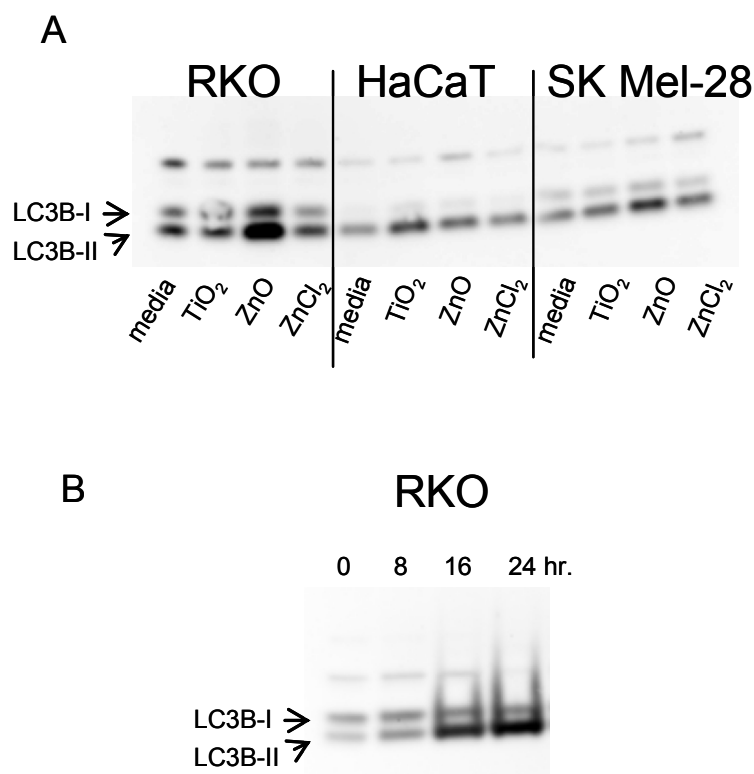


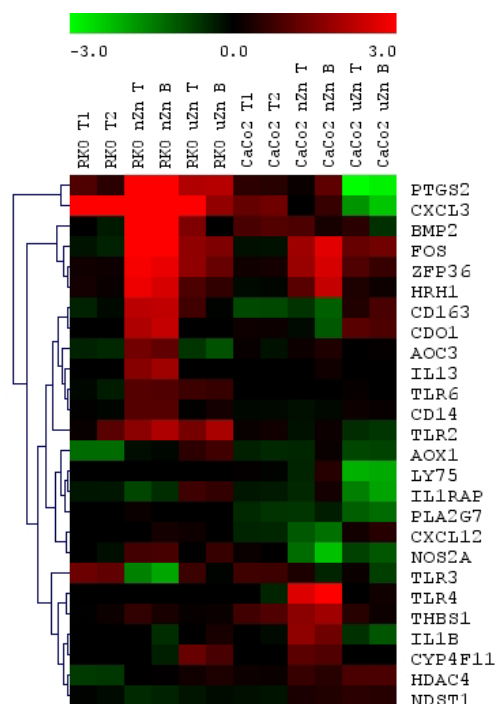
**Figure S4.** A) Zn and nanoparticulate treatment of RKO, HaCaT, SK-Mel 28 cells demonstrating LC3B cleavage in RKO and SK Mel-28 cells but minimal activation of LC3B in HaCaT cells. B) Time course study of nano-ZnO in RKO cells demonstrating LC3B cleavage.

The induction of LC3B in RKO and Sk Mel-28 cells is consistent with the increase in lysosomes observed above as well as the membrane structures visualized within the cells (figure 3).

### Microarray results: Inflammatory gene response.

We selected all the genes with Gene Ontology identifiers related to inflammation including: GO:0050727 (regulation of inflammation), GO:0006954 (inflammatory responses), GO:0006925 (inflammatory cell apoptosis), GO:0050729 (positive regulation of inflammatory response), or GO:0050728 (negative regulation of inflammatory response) as indicated by the annotation tables available from Agilent for the human whole genome array (of the 41000 unique probes, 315 probes were identified and used in this analysis). These data initially suggested there was not a cohort of genes that would be consistent with a pronounced pro-inflammatory signature. However, closer evaluation of select genes by evaluating differences among the RKO and CaCo-2 cell lines reveals that certain important pro-inflammatory genes were influenced by ZnO without activating entire signaling pathways. We observe that PTGS2 (also known as COX-2) message was elevated in RKO cells treated with nanoZnO compared with BSA-treated RKO cells but we do not observe this in CaCo-2 cells. In addition to PTGS2, another gene that appears to be expressed in a Zn-dependent manner and that is critical in the regulation of inflammation was ZFP36 (commonly known as tristetraprolin).

**Figure S5.** Hierarchical cluster visualization of inflammation-related transcript profiles in ZnO treated samples. Multiclass SAM was performed on the following categories 1) RKO, TNF- $\alpha$  pre-treatment, 2) RKO, nanoZnO treatment, 3) RKO microZnO treatment, 4) CaCo-2, TNF- $\alpha$  pre-treatment, 5) CaCo-2, nanoZnO treatment, and 6) CaCo-2, microZnO. 45 elements, representing 32 distinct probes, or 26 unique genes were highlighted in this analysis. Few genes consistently displayed expression changes indicating an inflammatory response.



### Quantitative PCR analysis

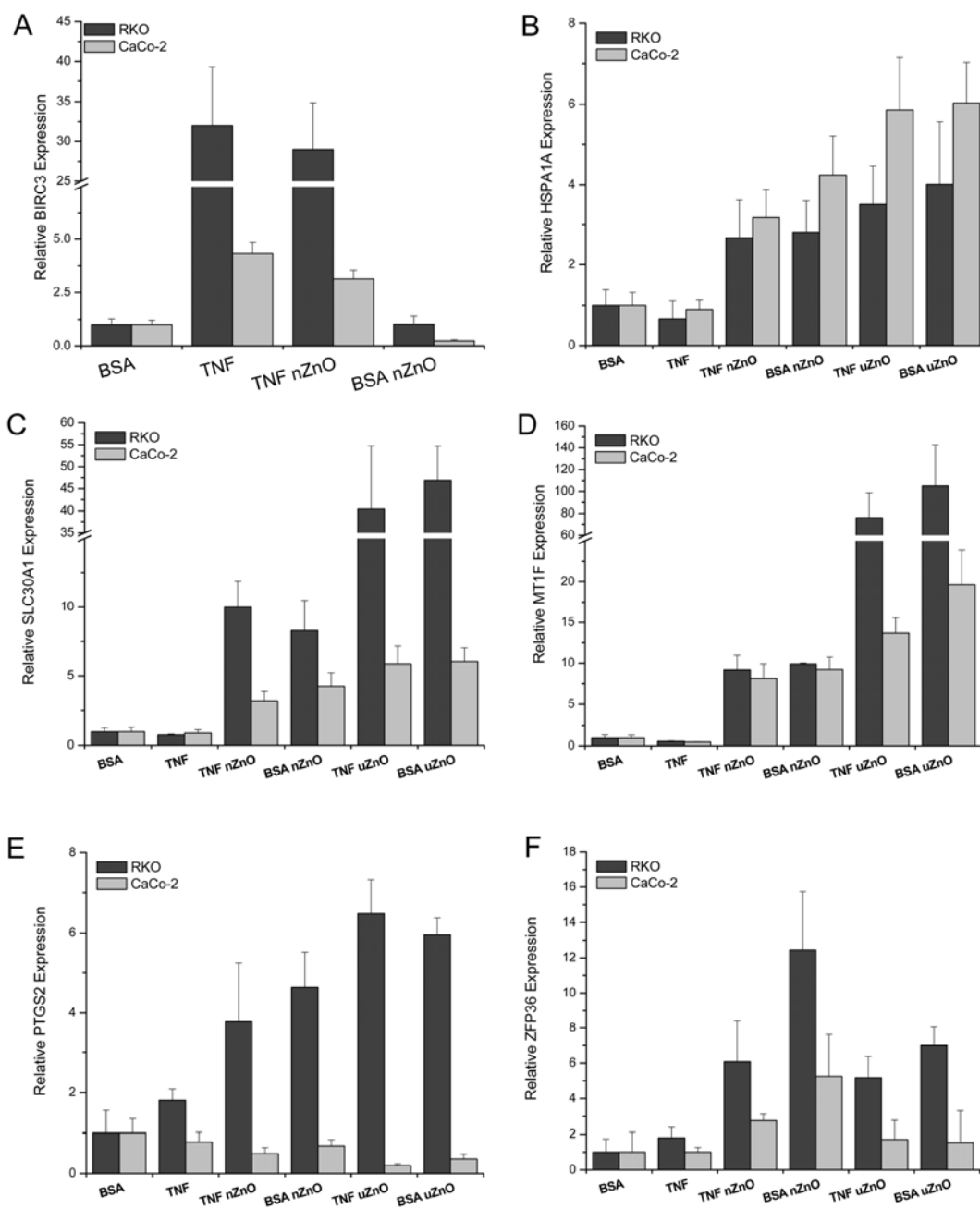
Quantitative PCR (QPCR) was performed to validate representative samples from the microarray analysis. For the QPCR, each biological replicate sample was evaluated individually. All amplicons were designed to be less than 150 bp in length, with primers that would anneal at about 60°C, and most span an intron of the gene of interest (if possible) in its genomic context. Primers sets were generated to evaluate the expression levels of BIRC3, HSPA1A, SLC30A1, MT1F, and ZFP36. B2M was used as the internal control to measure relative changes in expression. Primers used are listed in Primer Table S1 below.

**Table S1: Primers used for Q-PCR**

Gene Symbol	Forward Primer <sup>a</sup>	Reverse Primer
B2M	ttctggcctggaggetatc	tcaggaaatttgactttccattc
BIRC3	cttgctcttgctggtgcat	aagaagtcgtttctcctttgt
HSPA1A <sup>b</sup>	ggagtcctacgcctcaaca	ccagcaccttctcttgctg
PTGS2	cttcacgcacagttttcaag	tcaccgtaaatatgatttaagtccac
SCL30A1	gaccaggaggagaccaacac	caccacttctggggtttct
MT1F	tgettcttcgcttctctcttg	caggtgcaggagacacca
ZFP36 <sup>b</sup>	aagagaccccccagct	cccagacgctgataggagtg

<sup>a</sup>- all primers read 5' to 3'.  
<sup>b</sup>- does not span an intron.

Copy number standards were generated by cloning the amplicon of all PCR products except ZFP36 and PTGS2, into the pSC-A PCR system (Agilent). ZFP36 and PTGS2 standards were generated from a human open reading frame construct (ZFP36) or an expression vector (PTGS2) containing the coding sequences for these genes. Total RNA (1 µg) was used to generate first strand cDNA utilizing Superscript III (Invitrogen) and random nonamer primers (150 ng/reaction). The cDNA was diluted 1:60 in the final reaction mix that used SYBR Green I to evaluate relative expression among the experimental samples. Using the copy number standard curves, absolute quantification of the particular gene for each sample was calculated and the relative expression was calculated by dividing by the B2M level in the same sample. First, we measured the level of the TNF- $\alpha$ -regulated, anti-apoptotic gene, BIRC3, in the samples used in the initial analyses. We observed a clear induction of BIRC3 in samples pretreated with TNF- $\alpha$  compared to the cells pretreated with BSA (figure S6A). ZnO induced chaperon gene expression and we evaluated HSPA1A as a representative of this class of genes and confirmed the ZnO-dependence as TNF- $\alpha$  pretreatment did not alter gene expression (figure S6B). Cellular Zn metabolism and distribution genes also showed a pronounced effect of ZnO treatment, and therefore, we evaluated Zn efflux transporter, SLC30A1, and a metallothionein gene, MT1F (figures S6C & D). Interestingly, the conventional ZnO-treated RKO cells displayed more induction of these Zn metabolism genes than the nanoZnO-treated cells. Finally, we evaluated the expression of the inflammation related genes, PTGS2 and ZFP36. PTGS2 displayed cell type-specific differential expression on the microarrays when treated with ZnO particulate matter, and this was verified in the QPCR (figure S6E). Somewhat similar to PTGS2, ZFP36 displayed cell type differential expression; however, ZFP36 increases with nanoZnO treatment in both cells but is more pronounced in RKO cells compared to CaCo-2 cells (figure S6F). In all cases, the QPCR validated the direction of transcriptional changes observed on the microarrays, but the sensitivity of QPCR frequently demonstrated greater induction of these genes compared to the microarray.



t  
cell.

**Figure S6.** Validation of microarray expression results using quantitative PCR of 6 genes. **(A)** BIRC3 TNF- $\alpha$  responsiveness was evaluated in both cell lines with and without TNF- $\alpha$  and the nanoZnO samples were used as nanoparticulate treated samples. Protein unfolding responses were prominent so we evaluated HSPA1A as representative of this response. **(B)** HSPA1A demonstrated ZnO responsiveness, and no specific TNF- $\alpha$  response. Zn ion responsiveness was a prominent response so we validated MT1F and SLC30A1. **(C)** MT1F represents one of the metallothioneins that

were responsive to ZnO treatment. **D)** SLC30A1 is the Zn efflux transporter and demonstrates induction in the ZnO treated cells. Since we were interested in inflammatory responses, we evaluated PTGS2 and ZFP36. **E)** PTGS2 displayed one of the most complex expression patterns with respect to the ZnO treatments with respect to the two cell lines. **F)** ZFP36 demonstrated ZnO responsiveness. All of these genes were measured relative to the B2M expression in the same sample.

**Microarray results, hierarchical clusters of all genes identified as differentially expressed by SAM demonstrating ZnO cell contact gene expression changes:**

Multiclass SAM was performed on the following categories: 1) control samples, 2) ZnO contact treated samples, 3) TiO<sub>2</sub> treated samples, and 4) ZnCl<sub>2</sub> treated samples and the HaCaT ZnO Transwell sample where the cells were maintained separate from the cells. Using a false discovery rate of 0%, 274 elements, representing were identified. Reducing the gene set by repeated probes and genes left 122 genes that displayed differences among these groups. In this group, the samples are arranged so that the control samples (groups 1 & 3) are listed on the left, followed by the ZnO treated samples (group 2), and then the soluble Zn treatments are on the right (group 4). Gene expression of metal metabolism related genes still display enhanced expression while many others do not display altered expression from the untreated control comparison. Figure S7 displays the profiles of select sets of genes. The individual genes are not distinguished, instead, the figure delineates the profiles select sets of genes; 1) metal metabolism and 2) protein folding and stress response. The profiles demonstrate that samples without ZnO or soluble Zn treatments generally have low expression (on the left of both figures – with gene expression ratio close to 0 meaning that there is little difference between this condition and an untreated control), cells treated with ZnO have induced expression (the center of both figures – there are distinctions in magnitude among these cell lines but the expression ratio increases), and finally that soluble Zn is distinct between these sets of genes (the metal metabolic genes remain induced but the stress/protein folding genes are back at the baseline). These data indicate that the contact and uptake of the ZnO generates an explicit stress and protein folding response associated with its cytotoxicity.



responsiveness in all Zn treated samples (*left side of the graph*). B) Expression profiles for the protein folding stress responses including; ATF3, BAG3, DNAJA1, DNAJA4, DNAJB1, DNAJB4, DNAJB6, ERRF1, FOS, GADD454B, HSPA1A, HSPA1L, HSPA4L, HSPA6, and HSPH1, demonstrate responsiveness to ZnO when in contact but not when ZnCl<sub>2</sub> or ZnO is not in contact (HaCaT TW ZnO).